Original papers
Manufacturing processes and systems

УДК 621.486 DOI: 10.17277/jamt.2022.02.pp.149-158

Experimental study of an annular four-stage thermoacoustic engine with a traveling wave

© Ilya B. Gorshkov[a]✉, Vladimir V. Petrov[a]

[a] *Saratov State University (National Research University), 83, Astrahanskaya St., Saratov, 410012, Russian Federation*

✉ GoshX3@mail.ru

Abstract: In this paper a sample of an experimental annular four-stage thermoacoustic engine with a traveling wave was created in order to measure its performance, as well as to determine the optimal length of the cavities between the heat exchangers and the end surfaces of the stages. The engine stage diameter was 32 mm, the diameter of the resonators connecting the stages was 13 mm, and the total length of the ring resonator was 4.9 m. When thermal energy was supplied to the engine at a power of 88 W to 480 W, measurements of the amplitude distribution of pressure fluctuations in the resonator, acoustic power, and other parameters were made, in particular: electric heating power of each hot heat exchanger, pressure fluctuations at seven different points of the resonator, frequency of acoustic vibrations, temperature of each of the heat exchangers. In order to determine the optimal dimensions of the length of the cavities between the heat exchangers and the end surfaces of the stages, studies on the dependence of engine characteristics on the length of these cavities were carried out. It was shown that the optimal size of the cavities for a step with a diameter of 32 mm was in the range from 0 to 6 mm.

Keywords: acoustic self-oscillations; Delta EC program; regenerator; Stirling engine; thermoacoustics.

For citation: Gorshkov IB, Petrov VV. Experimental study of an annular four-stage thermoacoustic engine with a traveling wave. *Journal of Advanced Materials and Technologies*. 2022;7(2):149-158. DOI:10.17277/jamt. 2022.02.pp.149-158

Экспериментальное исследование кольцевого четырёхступенчатого термоакустического двигателя с бегущей волной

© И. Б. Горшков[a]✉, В. В. Петров[a]

[a] *Саратовский национальный исследовательский государственный университет имени Н. Г. Чернышевского, ул. Астраханская, 83, Саратов, 410012, Российская Федерация*

✉ GoshX3@mail.ru

Аннотация: Создан образец экспериментального кольцевого четырехступенчатого термоакустического двигателя с бегущей волной в целях измерения его рабочих характеристик, а также определения оптимальной длины полостей между теплообменниками и торцевыми поверхностями ступеней. Диаметр ступени двигателя составил 32 мм, диаметр соединяющих ступени резонаторов – 13 мм, суммарная длина кольцевого резонатора – 4,9 м. Экспериментальный образец двигателя не предусматривал акустической нагрузки, в качестве рабочего тела использовался воздух под атмосферным давлением. При подведении к двигателю тепловой энергии при мощности от 88 до 480 Вт проведены измерения распределения амплитуды колебания давления в резонаторе, акустической мощности, а также других параметров, в частности: электрической мощности нагрева каждого горячего теплообменника, колебания давления в семи различных точках резонатора, частоты акустических колебаний, температуры каждого из теплообменников. В целях определения оптимальных размеров длины полостей между теплообменниками и торцевыми поверхностями ступеней проведены исследования зависимости характеристик двигателя от длины этих полостей. Показано, что оптимальная величина полостей для ступени диаметром 32 мм находиться в диапазоне от 0 до 6 мм.

Ключевые слова: термоакустика; двигатель Стирлинга; регенератор; акустические автоколебания; программа Delta EC.

Для цитирования: Gorshkov IB, Petrov VV. Experimental study of an annular four-stage thermoacoustic engine with a traveling wave. *Journal of Advanced Materials and Technologies*. 2022;7(2):149-158. DOI:10.17277/jamt. 2022.02.pp.149-158

1. Introduction

A traveling wave thermoacoustic engine is an engine with an external heat supply. The engine converts thermal energy into acoustic energy due to the completion of a thermodynamic cycle that is closest to the Stirling cycle [1]. Unlike the Stirling engine, a thermoacoustic engine demonstrates the change in gas parameters: expansion, compression and movement from a hot heat exchanger to a cold one and vice versa, does not occur through the movement of pistons, but due to a traveling acoustic wave that occurs inside the engine. A wave occurs in such an acoustic generator at a resonant frequency determined by the sound speed ratio in the working medium (gas) to the engine housing (resonator) length value. The acoustic wave is generated from noise and is amplified at the resonant frequency due to the work done on the gas in the thermodynamic cycle, which is carried out in the regenerator and heat exchangers in the presence of a temperature difference between the heat exchangers. The acoustic energy obtained in this way can be converted into electricity, for example, using a linear converter [2], or a bidirectional turbine connected to an electric generator [3–7]. The result is a thermal power generator with a minimum number of moving parts and a thermal efficiency of about 30 % [8].

It was Peter Zeperli, who was the first researcher to realize that fluctuations in gas pressure and velocity in a Stirling engine were similar to pressure and velocity fluctuations in gas in a traveling acoustic wave [9]. In 1979, he proposed the design of a single-stage annular traveling wave thermoacoustic engine. In 2010, De Blok from the Dutch company Aster Thermoacoustics proposed a variant of a four-stage engine [10]. He increased the diameter of the heat exchangers and the regenerator relative to the diameter of the resonator in order to reduce the gas velocity in the regenerator area, and also increased the number of engine stages to four, thus improving weight and size and reducing the minimum temperature difference required to start the engine. The design of a multistage annular traveling wave engine has the best weight and size characteristics among all designs of thermoacoustic engines. For example, compared to engines with a standing wave, the internal volume of the resonator of an annular multistage engine turns out to be at least five times smaller, with a comparable output power [11].

The stages (heat exchangers) of a four-stage engine have a larger diameter than the acoustic resonators connecting them. For this reason, a transition must be made between the stage body and the resonator (in this work, a flat flange). A space (cavity) must be provided between this flange and the heat exchanger so that the gas flow can be evenly distributed over the entire cross section of the heat exchanger. The size of this cavity (its length) has a significant effect on the parameters of the thermoacoustic engine.

The purpose of this study is to determine the optimal length of the cavities between the heat exchangers and the end surfaces of the stage flanges.

2. Materials and Methods

2.1. Design development of a four-stage traveling wave engine

When creating an experimental setup, the scheme of a four-stage ring engine proposed by De Block [6] (Fig. 1) was taken as a basis.

Each of the stages consists of a hot heat exchanger, to which thermal energy is supplied; a cold heat exchanger, from which thermal energy is removed, and a regenerator, which is located between the heat exchangers. The regenerator realizes the thermoacoustic effect of acoustic wave amplification. The steps are connected to each other by means of pipes – acoustic resonators, the length of which determines the resonant frequency of the excited vibrations.

Figure 3 shows a schematic representation of the stage of the developed experimental sample of the thermoacoustic engine.

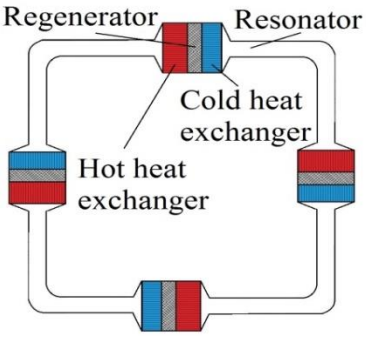

Fig. 1. Four-stage traveling wave engine

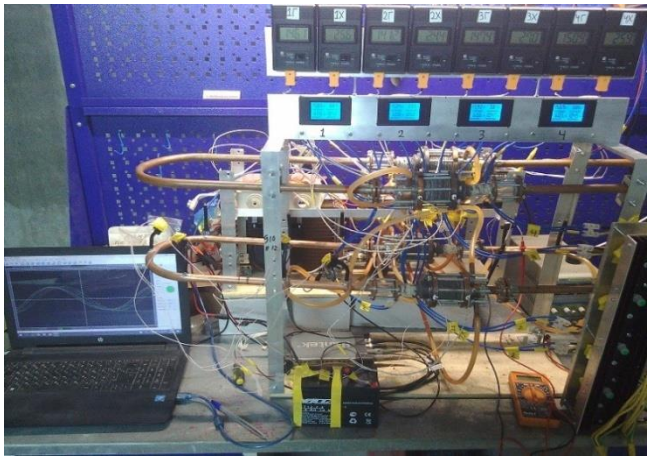

Fig. 2. Installation outer view

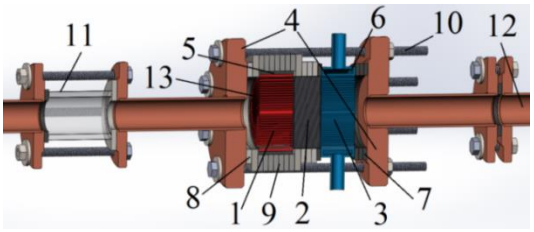

Fig. 3. Stage of the experimental engine in section:
1 – hot heat exchanger; 2 – regenerator; 3 – cold heat exchanger; 4 – connecting flanges; 5 – nichrome heater coil; 6 – cylindrical channel for coolant; 7 – paronite gasket – separator; 8 – asbestos gasket – separator; 9 – asbestos gaskets – heat insulators; 10 – bolted connections; 11 – quartz glass tube; 12 – resonator; 13 – thermocouple connection point

2.2. Development of the heat exchanger design

One of the main tasks set when constructing the engine design was to ensure the technological possibility of quick replacement and resizing of the heat exchanger, as well as changing its position inside the stage. For this purpose, most of the stage body in places with low temperatures was made up of paronite gaskets, and in places with high temperatures – from gaskets made of asbestos cushion cardboard. The resulting stack of gaskets and heat exchangers was clamped between the flanges using bolted connections to fix the structure and make it tight. By changing the number of gaskets, it was possible to change the length of the stage body in the required place and, thereby, change the location of the heat exchangers inside the stage. The developed design is aimed to work with gas at atmospheric pressure inside the engine. Figure 4 shows a cold heat exchanger in section.

The heat exchanger consists of copper plates bent in an Archimedes spiral for one turn. This shape of the plates is designed to provide a more uniform distribution of gas flows over the cross-sectional area of the heat exchanger and thus increase its thermal power. In this case, the distance between the plates in the central part differs from the distance between the plates on the periphery of the heat exchanger by no more than 15 %. Due to the small diameter of the heat exchanger (32 mm), it was possible to implement the removal and supply of thermal energy through its side surface. In a cold heat exchanger, spiral plates are inserted into an annular channel through which coolant (water) flows. These plates are connected to the channel with a layer of high-temperature sealant “Grey 999 gasket maker” with

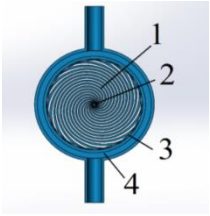

Fig. 4. Cold heat exchanger in section:
1 – spiral plates; 2 – a rod that closes the hole between the plates in the center; 3 – a sealant layer that fastens the plates; 4 – a cylindrical channel for water circulation

a thickness of about 0.5 mm. The sealant fixes the plates and also improves the thermal contact between the plates and the cooling channel.

The design of the hot heat exchanger is similar to the design of the cold one, however, instead of the cooling channel along the perimeter, there is a heating coil made of nichrome wire. To provide thermal insulation, the hot heat exchanger is placed inside a stack of asbestos spacer board gaskets. In order to reduce heat losses through the resonator housing, a quart glass insert with a length of 30 mm and an inner diameter of 17 mm was made on the side of the hot heat exchanger. The regenerator is a stack of 30 stainless steel meshes with a wire diameter of 0.2 mm and a wire spacing of 0.67 mm. Each of the four resonators connecting the stages is a round copper tube with an inner diameter of 13 mm, bent exactly in the middle by 180 degrees with a bend radius of 205 mm. The length of the curved section is 322 mm and the length of the straight sections is 828 mm. In total, the length of the resonator from the inner surface of the hot flange of one stage to the inner surface of the cold flange of the other stage is 1.15 meters. The total length of the entire ring resonator is 4.9 meters (Fig. 5).

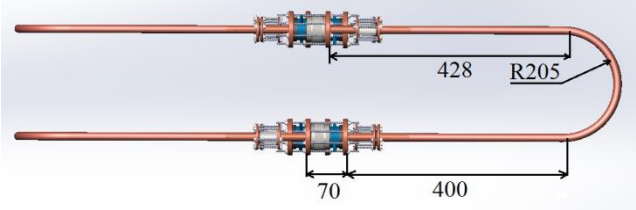

Fig. 5. Resonator dimensions

2.3. Determining the dependence of engine parameters on the length of the cavities between the heat exchangers and the stage connecting flanges

The purpose of the study is to determine the minimum length of the cavities between the heat exchangers and the end surfaces of the stage flanges (Fig. 6) in order to find their optimal dimensions. The cross-sectional area of the stage housing is larger than the cross-sectional area of the resonator. As mentioned earlier, this was done to reduce viscous losses in the heat exchanger and improve weight and size characteristics. In this case, when gas flows from the resonator cavity into the stage cavity and back, additional hydraulic losses occur due to a sharp change in the housing diameter [12]. In addition, there is a non-uniformity of the oscillatory velocity of the gas in the heat exchangers over their cross-sectional area. In the center of the heat exchanger, the vibrational velocity is greater, and less along the perimeter. To reduce the non-uniformity of vibrational velocity in heat exchangers and reduce hydraulic losses, the transition between small and large diameters is made in the form of a cone [13], or an additional space (cavity) is made between the end surface of the stage and the heat exchanger [14].

For the numerical calculation of thermoacoustics equations, there is a Delta EC program. This program can take into account turbulent effects in pipes and cones, but it is impossible to simulate the uneven distribution of vibrational velocity over the cross section of heat exchangers and the related effects [15]. In this regard, the task was to determine the dependence of the engine parameters on the length of the cavities between the heat exchangers and the connecting flanges of the stage. If the heat exchangers are located close to the flanges in the absence of cavities, then the non-uniformity of the vibrational velocity in them will be maximum. With an increase in the length of the cavities, the unevenness of the vibrational speed decreases and the heat exchangers work more efficiently. However, there is some optimal value of this length, since with its further increase, the generated power decreases, and the weight and size indicators of the system as a whole also deteriorate [16].

Air at atmospheric pressure was used as the working fluid in the engine. In all experiments, the engine was operated without acoustic loading. The parameters of the developed experimental engine are presented in Table 1.

The porosity of heat exchangers is the ratio of the cross-sectional area occupied by the gas to the total cross-sectional area of the heat exchanger. In this experiment, the thickness of the heat exchanger plates and the distance between the plates are equal to each other, so the porosity was found to be 0.5. The porosity of the regenerator was calculated by the formula [15]:

$$\phi = 1 - \frac{\pi\, m\, d_{\text{wire}}}{4}, \qquad (1)$$

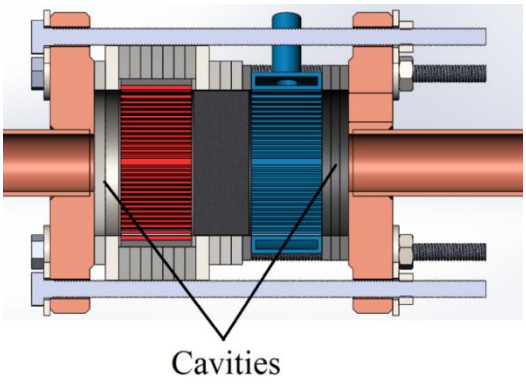

Fig. 6. Location of the studied cavities

Table 1. Parameters unchanged during the experiments

Element	Diameter, mm	Length, mm	Porosity	Hydraulic radius, mm	Distance between plates
Hot heat exchanger					
Cold heat exchanger	32	16	0.5	–	0.5
Regenerator	33	12.5	0.766	0.164	–
Resonator	13	1150	1	3.250	

here m is the number of wires per unit length of the mesh, let us say per meter, then d_{wire} is wire diameter in meters.

The hydraulic radius of the regenerator was calculated by the formula [14]:

$$r_h = d_{\text{wire}} \frac{\phi}{4(1-\phi)}. \quad (2)$$

The thermal penetration depth δ_k in the experiments was taken equal to 0.38 mm, and the viscous penetration depth δ_υ was about 0.32 mm. Thus, the hydraulic pore radius of the regenerator turned out to be 2.3 times less than δ_k.

During the experiments, the following parameters were measured: electric heating power of each hot heat exchanger (using four wattmeters "Peacefair DC 6.5 – 100 V"); pressure fluctuations at seven different points of the resonator, as well as the frequency of acoustic oscillations (using differential pressure sensors "MPX5050DP"); temperature of each of the heat exchangers (using eight K-type thermocouples connected to TM-902C electronic thermometers). The thermocouples were attached to the heat exchangers with a high-temperature sealant "Grey 999 gasket maker" exactly in the middle between their center and the outer diameter on the opposite side of the regenerator.

The experiments were carried out for four different distances between the heat exchangers and the connecting stage flanges. The distance was changed (increased) by increasing the number of asbestos gaskets on the hot side and paronite gaskets on the cold side between the heat exchangers and flanges (Table 2).

Table 2. Distances between the end surfaces of the stage (flanges) and heat exchangers in experiments

Parameter	Experiments			
	1	*2*	*3*	*4*
Distance between hot heat exchanger and flange $L_{n\,\text{hot}}$, mm	6	8,5	11	13,5
Distance between cold heat exchanger and flange $L_{n\,\text{cold}}$, mm		8	10	12

In experiment *1*, the temperature of heat exchangers and pressure fluctuations were measured at 10 different values of the input thermal power of the engine W_{therm}, in the range from 88.8 to 480.4 W. In experiments *2*, *3* and *4*, the measurements were carried out at 3 different values of the input thermal power in the same range. When changing the input heat power W_{therm}, it is necessary to provide some time to achieve the heat balance of the entire system. To determine the state of the heat balance for a given thermal power W_{therm}, the measurements were carried out first with a successive increase in the thermal power, and then with a decrease, passing through the same values W_{therm}. Between two successive measurements, a pause of 25 minutes was made to approach the heat balance. During this pause, measurements of the engine parameters were carried out with an interval of 5 minutes. Figure 7 shows an example of such a measurement.

The temperature at which the heat balance occurs was taken as the average temperature between the upper and lower values on the graph (Fig. 7) at the time of 25 minutes.

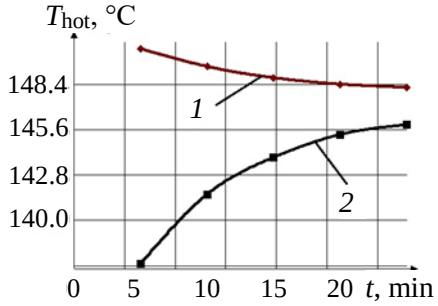

Fig.7. The temperature of the hot heat exchanger when approaching the heat balance (graph *1* – when passing "down", graph *2* – when passing "up")

3. Results and Discussion

Pressure fluctuations were measured using 7 sensors located on one of the resonators at distances of 155, 265, 435, 585, 735, 910, and 1020 mm from the end surface of the stage on the side of the hot heat exchanger.

Figure 8 shows the characteristic distribution of the amplitude of pressure oscillations $|P_1|$ along the length of the resonator. A similar distribution was observed in [17–20].

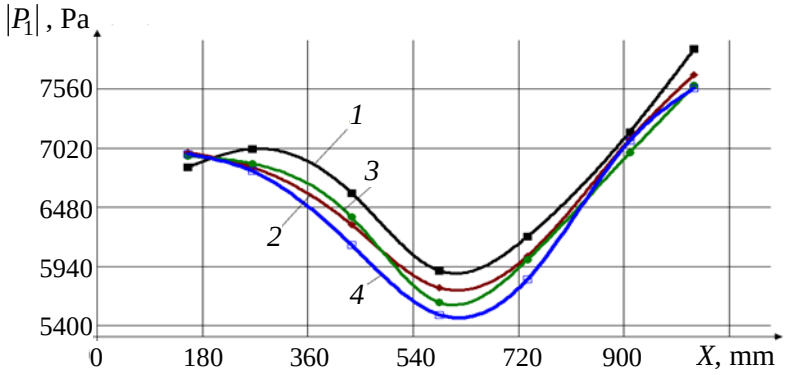

Fig. 8. Distribution of the amplitude of pressure oscillations $|P_1|$ along the length of the resonator X in different experiments (*1*, *2*, *3*, *4* – serial numbers of experiments)

The power of the thermal energy supplied to the engine was 480 W, the temperature of the hot heat exchangers was $T_{\text{hot}} = 230$ °C, and that of the cold heat exchangers was $T_{\text{cold}} = 70$ °C. The amplitude of pressure fluctuations on the side of the hot heat exchanger turned out to be smaller than on the side of the cold heat exchanger. In addition, there is an amplitude dip in the central part of the resonator. In the presence of a traveling wave in the resonator, one would expect a gradual decrease $|P_1|$ as the distance from the hot heat exchanger increases due to the attenuation of the wave as it propagates through the resonator. However, this was not observed in this experiment. The real distribution $|P_1|$ is explained by the fact that the phase difference between the velocity and pressure fluctuations in the resonator is not equal to 0 degrees as in a traveling wave, but reaches values of 35 degrees (according to the results of calculations in Delta EC), that is, this is the sum of traveling and standing waves. The standing component arises when the wave is reflected from the surfaces of the heat exchangers and the end surfaces of the steps. The traveling wave is present only inside the engine stages.

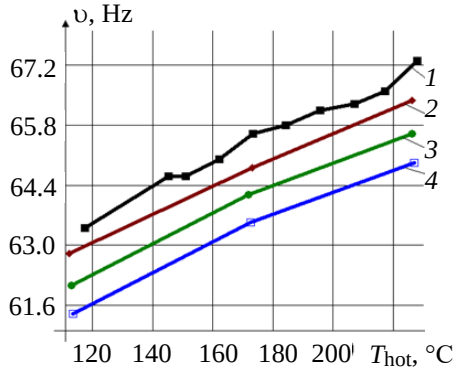

Fig. 9. Dependence of the oscillation frequency υ on the average temperature of hot heat exchangers T_{hot} (*1*, *2*, *3*, *4* – serial numbers of experiments)

The frequency of acoustic vibrations depends on the length of the engine casing. For a wave propagating in an annular waveguide of constant cross section and without heat exchangers inside, the oscillation frequency can be calculated by dividing the speed of sound in the gas by the length of the casing. It is possible to carry out such an estimated calculation for this engine. The speed of sound in air at an average temperature in the engine of 90 °C is 382, the body length is 4.9 m. The oscillation frequency is 78 Hz.

The measured values are shown in Fig. 9. It can be seen that the presence of heat exchangers inside the housing, as well as the thickening of the housing at the places where the heat exchangers are installed, reduce the oscillation frequency υ relative to the estimated frequency of 78 Hz to values of 63.4–67.3 Hz. An increase in υ with an increase in the temperature of hot heat exchangers is due to an increase in the average air temperature in the engine and, accordingly, an increase in the speed of sound in it. In each subsequent experiment, the oscillation frequency decreased due to an increase in the body length due to an increase in the distances $L_{n\text{hot}}$ and $L_{n\text{cold}}$ between the heat exchangers and the stage flanges.

The acoustic wave power in the resonator was calculated using the Delta EC program. This program was used to integrate the equations of thermoacoustics for the resonator.

$$\frac{dP_1}{dx} = -(i\,\omega\, l + r_v)\, U_1; \qquad (3)$$

$$\frac{dU_1}{dx} = -\left(i\,\omega\, c + \frac{1}{r_k}\right) P_1. \qquad (4)$$

Here $P_1 = P_1(x)$ is a complex number depending on the coordinate *x*. The same is true for volume flow U_1. The modulus of the number $|U_1|$ is equal to the amplitude of volume flow fluctuations at a given point, and the phase U_1 is equal to the phase of pressure fluctuations at a given point; i is the imaginary unit, ω is the circular frequency of oscillation, l is the acoustic inertia per unit length, which reflects the inertial properties of the gas in a given engine structural element, c is the acoustic compliance per unit length, which reflects the elastic properties of the gas in a given structural element, r_v is the viscous resistance, which leads to loss of energy for friction, r_k is thermal resistance, which leads to loss of energy due to thermal interaction with the surface of the element.

To calculate the power $|P_1|$, it is necessary to know the amplitudes of pressure fluctuations and volume flow $|U_1|$, as well as the phase difference Δφ between pressure and volume flow fluctuations. Suppose that the amplitude of pressure fluctuations at a given point is known (measured using a pressure sensor), then $|U_1|$, Δφ remain unknown. Parameters l, c, r_v, r_k in equations (3), (4) can be calculated knowing the physical properties of the gas, the resonator diameter and the frequency of acoustic oscillations. It turns out a system of two equations (3) and (4) with two unknowns. Knowing the pressure amplitudes at two other points of the resonator and substituting them as the boundary conditions of the system of equations, this system is simply solved. To solve it numerically, the following target parameters and variables are used in the Delta EC program: reference pressure P_m, oscillation frequency υ, gas temperature in the resonator and its geometric dimensions, as well as the amplitude of pressure oscillations at 3 points of the resonator. Three amplitudes of pressure fluctuations are the purpose of the calculation, and the initial amplitude of pressure fluctuations, volume flow, and phase difference are variable parameters. Thus, using the results of measurements from three pressure sensors, it is possible to calculate the power of an acoustic wave, taking into account friction losses, thermal relaxation for any phase difference between pressure and gas velocity fluctuations. The accuracy of this method should increase with increasing distance between the sensors. For this reason, in this work, data from the outer sensors on the resonator and from the middle sensor were used for calculations. The calculation results are shown in Fig. 10.

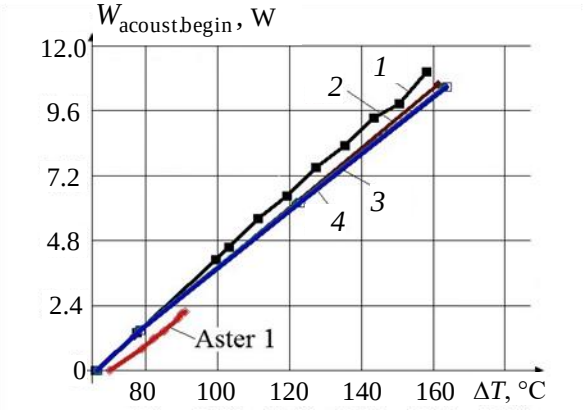

Fig. 10. Dependence of the acoustic power at the beginning of the resonator $W_{acoust.begin}$ (at the outlet of the hot heat exchanger) on the average temperature difference between hot and cold heat exchangers ΔT (*1*, *2*, *3*, *4* – serial numbers of experiments; aster 1 is a graph built on the basis of data from the article [6])

Dependence $W_{acoust.begin}$ on ΔT is linear. The maximum acoustic wave power was observed in the first experiment at distances between heat exchangers and end flanges equal to 6 mm and reached 11 W at $\Delta T = 158$ °C. As these distances increased, the acoustic power decreased.

To compare the results with the data of other authors, the work [10] was used, in which a similar engine was studied, except for the size and some other features. Engine power is proportional to the cross-sectional area of the heat exchangers. The cross-sectional area of the heat exchangers and the regenerator of the engine in the article [10] is 28 times larger than the area of the engine under study. Therefore, in order to compare a larger engine with a smaller engine, the power of the large engine was divided by 28 and shown in fig. 10.

The engine, indicated on the graph as Aster 1, has less power per unit area of the cross-sectional area of heat exchangers over the entire temperature range, most likely due to the fact that in this engine automobile radiators were used as heat exchangers, in which the distance between the plates is much greater than 0.5 mm (much larger than the heat exchangers in this work). In addition, the hydraulic radius of the regenerator for the Aster engine is 50 μm, that is, 7.6 times less than δ_k, which increases the viscosity losses compared to the engine studied in this work.

The efficiency of converting thermal energy into acoustic energy was calculated as the ratio of the acoustic wave power at the beginning of the resonator (behind the hot heat exchanger) $W_{acoust.begin}$ to the thermal power supplied to the engine W_{therm}.

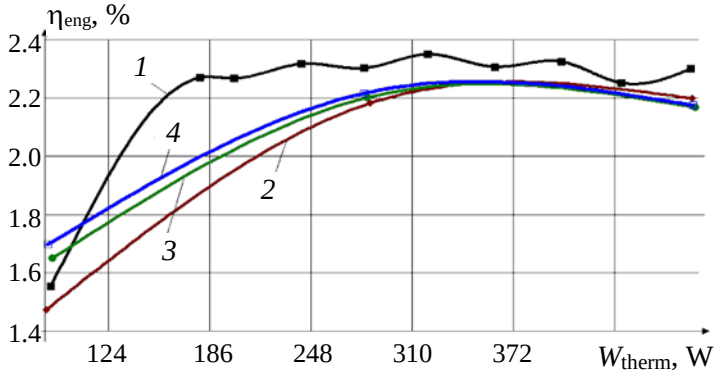

Fig. 11. Dependence of acoustic efficiency η_{eng} on the supplied thermal power W_{therm} (*1*, *2*, *3*, *4* – serial numbers of experiments)

Since in experiment *1* 10 measurements were carried out with different thermal power W_{therm}, and in experiments *2*, *3* and *3*, 3 measurements each, then the shape of the curve for the first experiment in Fig. 11 is noticeably different from the rest.

When analyzing the graph corresponding to experiment *1*, it can be seen that with an increase W_{therm} to 180 W, the efficiency increases, and then the growth stops at around η_{eng} = 2.3 %. The cessation of the efficiency increase can be explained by the fact that as the input thermal power increased, the temperature of not only hot heat exchangers, but also cold ones increased, which led to a decrease in the theoretically maximum possible thermal efficiency. Such a small efficiency value of 2.3 % is typical for engines operating with atmospheric pressure of the working fluid. With an increase in pressure inside the engine, the power of the acoustic wave increases at a fixed temperature difference, and the power of heat losses through the casing, through the regenerator and into the environment remains the same as at atmospheric pressure. Thus, with an increase in pressure, the proportion of heat loss power relative to acoustic power decreases and the efficiency increases [10].

4. Conclusions

In this paper, the parameters of a four-stage traveling-wave thermoacoustic engine were studied for various values of the supplied thermal power and for various sizes of cavities between the heat exchangers and the end surfaces of the stage body. The main goal was to determine the optimal size (length) of these cavities. Measurement with cavity sizes less than 6 mm was not possible due to the design features of the heat exchangers. As the length of the cavities increased, the acoustic power decreased. As it was later found out, the decrease in power was due to the fact that the cavities in each subsequent experiment not only increased in length, but also increased the difference between the lengths of the cavities behind the hot heat exchanger and behind the cold heat exchanger (see Table 2). If in the first experiment the lengths of the cavities $L_{n\,hot}$ and $L_{n\,cold}$ were equal, then in the second experiment the difference between them was already 6.25%, in the third 10 %, and in the fourth 12.5 %. The differences between the lengths $L_{n\,hot}$ and $L_{n\,cold}$ of the cavities led to the fact that the heat exchanger began to leave the region with the maximum acoustic impedance and the acoustic power fell. The value of the drop in acoustic power due to the displacement of the heat exchanger from the zone of maximum acoustic impedance was the largest in the fourth experiment and amounted to 11.3 % relative to the first experiment.

The cross-sectional area of the heat exchangers is 6 times larger than the cross-sectional area of the resonator. For this reason, a strong (several times) decrease in the acoustic power was expected with a decrease in the length of the cavities $L_{n\,hot}$ and $L_{n\,cold}$ due to an increase in the distribution inhomogeneity of the vibrational velocity over the heat exchanger cross-sectional area. However, in the experiment, up to a cavity length of 6 mm, no decrease in acoustic power was recorded. Thus, we can conclude that the optimal size of the cavities for a step with a diameter of 32 mm is in the range from 0 to 6 mm for a given design of heat exchangers and the entire engine as a whole.

An acoustic wave was observed in the engine resonator, which is the sum of the traveling and

standing wave components. A standing wave has a pressure node at the center of the resonator and an antinode at the boundary with the heat exchanger. The maximum efficiency of converting thermal energy into electrical energy (2.3 %) was observed at a thermal power supplied to the engine of about 340 W. Such low efficiency is typical for devices operating with atmospheric pressure of the working fluid. By increasing the average pressure in the cycle, the efficiency of the thermoacoustic engine can be significantly increased.

5. Funding

The research leading to these results received funding fromthe Russian Foundation for Basic Research under Grant Agreement No. 19-32-90127.

6. Conflict of interests

The authors declare no conflict of interest.

References

1. Swift GW. *Thermoacoustic engines and refrigerators: a short course*. Los Alamos: Los Alamos National Laboratory; 1999. 179 p.

2. Yu Z, Jaworski A, Backhaus S. Travelling-wave thermoacoustic electricity generator using an ultra-compliant alternator for utilization of low-grade thermal energy. *Applied Energy*. 2012;99:135-145. DOI:10.1016/j.apenergy.2012.04.046

3. Dovgjallo AI, Shimanov AA. Possibility of using a bi-directional impulse turbine in a thermo-acoustic engine. *Vestnik Samarskogo Gosudarstvennogo Aerokosmicheskogo Universiteta*. 2015;14(1):132-138. DOI:10.18287/1998-6629-2015-14-1-132-138 (In Russ.)

4. Timmer MAG, de Blok K, van der Meer TH. Implementing a bidirectional impulse turbine into a thermoacoustic refrigerator. *The Journal of the Acoustical Society of America*. 2020;148(3):1703-1712. DOI:10.1121/10.0002001

5. Timmer MAG, van der Meer TH. Characterization of bidirectional impulse turbines for thermoacoustic engines. *The Journal of the Acoustical Society of America*. 2019;146(5):3524-3535. DOI:10.1121/1.5134450

6. Timmer MAG, van der Meer TH. Optimizing bidirectional impulse turbines for thermoacoustic engines. *The Journal of the Acoustical Society of America*. 2020;147(4):2348-2356. DOI:10.1121/10.0001067

7. Liu D, Chen Y, Dai W, Luo E. Acoustic characteristics of bi-directional turbines for thermoacoustic generators. *Frontiers in Energy*. 2020:1-10. DOI:10.1007/s11708-020-0702-3

8. Bi T, Wu Z, Zhang L, Yu G, Luo E, Dai W. Development of a 5 kW traveling-wave thermoacoustic electric generator. *Applied Energy*. 2017;185:1355-1361. DOI:10.1016/j.apenergy.2015.12.034

9. Ceperley PH. A pistonless Stirling engine – the traveling wave heat. *The Journal of the Acoustical Society of America.* 1979;66(5):1508-1513. DOI:10.1121/1.383505

10. Blok K. Novel 4-stage traveling wave thermoacoustic power generator. *Proceedings of ASME 2010 3rd joint US-European fluids engineering summer meeting and 8th international conference on nanochannels, microchannels, and minichannel, 1-5 August 2010.*Monreal, Canada: 2010. p. 73-79. DOI:10.1115/FEDSM-ICNMM2010-30527.

11. Blok K. *Multi-stage traveling wave thermoacoustic in practice.* Available from: https://citeseerx.ist.psu.edu/viewdoc/download?doi=10.1.1.454.1398&rep=rep1&type=pdf [Accessed 09 February 2022]

12. Smith BL, Swift GW. Power dissipation and time-averaged pressure in oscillating flow through a sudden area change. *The Journal of the Acoustical Society of America*. 2003;113(5):2455-2463. DOI:10.1121/1.1564022

13. Kruse A, Schmiel T, Tajmar M. Experimental validation of a looped-tube thermoacoustic engine with a stub for tuning acoustic conditions. *Energy Conversion and Management*. 2018;177:292-305. DOI:10.1016/j.enconman.2018.09.069

14. Kruse A, Ruziewicz A, Tajmar M, Gnutek Z. A numerical study of a looped-tube thermoacoustic engine with a single-stage for utilization of low-grade heat. *Energy Conversion and Management*. 2017;149:206-218. DOI:10.1016/j.enconman.2017.07.010

15. Ward B, Clark G, Swift G. *Design environment for low-amplitude thermoacoustic energy conversion, version 6.3b11, users guide.* Los Alamos: Los Alamos National Laboratory; 2012. 288 p.

16. Petrov VV, Gorshkov IB. Numerical simulation of a looped tube 4-stage traveling-wave thermoacoustic engine. *Izvestiya of Saratov University. New Series. Series: Physics*. 2018;18(4):285-296. DOI:10.18500/1817-3020-2018-18-4-285-296 (In Russ.)

17. Yang R, Meir A, Ramon GZ. Theoretical performance characteristics of a travelling-wave phase-change thermoacoustic engine for low-grade heat recovery. *Applied Energy.* 2020;261:1-11. DOI:10.1016/j.apenergy.2019.114377

18. Hamood A, Jaworski A, Mao X. Development and assessment of two-stage thermoacoustic electricity generator. *Energies.* 2019;12(9):1-18. DOI:10.3390/en12091790

19. Hamood A, Jaworski A. Experimental investigations of the performance of a thermoacoustic electricity generator. *ASEE19 E3S Web of Conferences.* 2019;116:1-8. DOI:10.1051/e3sconf/201911600025

20. Abdoulla-Latiwish KOA, Jaworski AJ. Two-stage travelling-wave thermoacoustic electricity generator for rural areas of developing countries. *Applied Acoustics.* 2019;151:87-98. DOI:10.1016/j.apacoust.2019.03.010

Information about the authors / Информация об авторах

Ilya B.Gorshkov, Postgraduate Student, Saratov State University (National Research University), Saratov, Russian Federation; ORCID 0000-0003-0183-769X; e-mail: GoshX3@mail.ru

Vladimir V. Petrov, D. Sc. (Phys. and Math.), Professor, Saratov State University (National Research University), Saratov, Russian Federation; ORCID 0000-0002-8520-5245; e-mail: petrovvv@sgu.ru

Горшков Илья Борисович, аспирант, Саратовский национальный исследовательский государственный университет имени Н. Г. Чернышевского, Саратов, Российская Федерация; ORCID 0000-0003-0183-769X; e-mail: GoshX3@mail.ru

Петров Владимир Владимирович, доктор физико-математических наук, профессор, Саратовский национальный исследовательский государственный университет имени Н. Г. Чернышевского, Саратов, Российская Федерация; ORCID 0000-0002-8520-5245; e-mail: petrovvv@sgu.ru

Received 14 March 2022; Accepted 20 May 2022; Published 01 July 2022